Deep-Sea Research I, Vol. 40, No. 11/12, pp. 2217–2228, 1993.
Printed in Great Britain.

0967–0637/93 $6.00 + 0.00

Seasonal and interannual variability of sea surface temperatures in the tropical Pacific, 1969–1991

THIERRY DELCROIX*

(*Received* 7 *December* 1992; *in revised form* 29 *April* 1993; *accepted* 29 *April* 1993)

Abstract—Water sample data derived from a ship-of-opportunity program are used to describe changes in sea surface temperature (SST) for the tropical Pacific. Time series up to 23 y long (1969–1991) allow investigation of both seasonal and interannual SST variability along four selected shipping tracks crossing the equator near 155°E, and 160, 140 and 100°W. Poleward of 6–8° latitude, the seasonal variability increases, reflecting the growing impact of surface thermal forcing. Within 6–8° latitude, the seasonal and interannual variabilities in the eastern Pacific are of the same order of magnitude, whereas in the western Pacific the interannual variability is 2–10 times greater than the seasonal variability. Maximum interannual variability appears trapped at and along the equator, in relation with the occurrence of El Niño (1976, 1982–1983, 1987 and 1991) and La Niña (1988–1989) events. Complementing various other local investigations, the present study enables basin-scale SST changes to be documented in a concise fashion.

INTRODUCTION

SEA surface temperature (SST) is probably the most complex physical oceanic parameter. Observing, understanding and ultimately predicting its variability is of major importance because SST anomalies are related to several aspects of the global climate (e.g. PAN and OORT, 1983; PALMER and MANSFIELD, 1984). Anomalies in SST are governed by various processes, which not only vary at different time and space scales, but are also closely dependent on each other: changes in SST involve multiple-scale coupled ocean–atmosphere interactions. Basically, SST is modified by two types of processes: those acting through the sea surface and those acting within the water mass. These processes include: (i) the net surface flux of solar energy, latent and sensible heat, and infrared radiation, and (ii) the horizontal and vertical advections and mixing by various scales of motion.

In extra-tropical regions, the surface thermal forcing is thought to control low-frequency SST changes, in contrast with tropical regions where the role of ocean dynamics cannot be dismissed. In the tropics, furthermore, the ocean–atmosphere coupling is enhanced, because the surface thermal forcing is influenced by atmospheric parameters (cloud, wind speed, air temperature, humidity, etc.), all of which are related to SST, and vice versa. Quantifying the relative contribution of processes that cause SST anomalies is thus a fascinating challenge; it underlies the international 1985–1994 Tropical Ocean and Global Atmosphere (TOGA) program (WORLD CLIMATE RESEARCH PROGRAM, 1985).

*Institut Français de Recherche Scientifique pour le Développement en Coopération (ORSTOM), Groupe SURTROPAC—Centre ORSTOM de Nouméa, BP A5 Nouméa, New Caledonia.

What do we know about SST changes at seasonal and interannual time scales, in the tropical Pacific? With the large body of scientific literature dealing with SST, one might be tempted to assume this parameter to be fairly familiar to us. However, papers include comprehensive descriptions based on atlases and real-time SST products (e.g. LEVITUS, 1982; REYNOLDS, 1988), regional descriptions relying on different types of instrumentation (XBT, moorings, drifting buoys, etc.) for various time periods (e.g. WHITE *et al.*, 1985; HAYES *et al.*, 1991; MCPHADEN *et al.*, 1992), and attempts to model and understand the SST climatology or its variability (e.g. SEAGER *et al.*, 1988; SEAGER, 1989). Consequently, with information about SST stemming from such a wide variety of sources, instruments, locations and time periods, it is often difficult to pinpoint differences and similarities between findings and to obtain a synthetic view.

The present approach complements other analyses by concentrating on basin-scale SST changes measured with the same technique, over a 23 y period. Specifically, this study is an investigation into the seasonal and interannual SST variations, from 1969 to 1991, as inferred from sea water samples collected along merchant ship routes. Obviously, some of the results will be familiar to the reader. However, as noted above, it is useful to document SST variations in a concise fashion. This is expected to highlight basin-scale SST features at seasonal and interannual time scales, and to facilitate comparisons with ocean–atmosphere model results.

The paper is organized as follows. Section 2 describes the measurements, the resulting data set and data processing. In section 3, emphasis is placed upon the mean and seasonal variability of SST. Then, in section 4, we focus on the SST signature of several El Niño (1976, 1982–1983, 1987 and 1991) and La Niña (1988–1989) events that strongly modified the physical environments throughout the Pacific basin.

THE DATA

The bulk of this work is based on an ongoing ship-of-opportunity program (SOP) developed and operated jointly by the ORSTOM centres in Nouméa (New Caledonia), and Papeete (French Polynesia) since 1969 and 1976, respectively. Among the various parameters gathered by this program, SST measurements are obtained from sea water samples in buckets collected along trans-Pacific routes every 55–110 km (about 25% of the 1969–1972 SST data came from intake measurements but this will not affect the main conclusions). The buckets are hauled up on to the bridge, and SST measurements are performed by volunteer ship officers by means of a Maurer–Amarell thermometer fitted inside the bucket (manufactured by Eurolabo, in Behren lès Forbach, France). The graduation interval for the thermometer is 1°C; one quarter of a degree is probably the minimum that can be estimated.

Out of all the SST measurements available for the tropical Pacific, I have selected about 139,000 observations along four well-sampled shipping tracks, during the 1969–1991 period (Fig. 1). For brevity, the tracks will be referred to as the western track, from 166°E–28°S to 142°E–28°N, the central track, from 166°E–28°S to 126°W–28°N, the east-central track, from 152°W–28°S to 126°W–28°N, and the eastern track, from 180°–28°S to 80°W–7°N.

The ORSTOM–SOP measurements were routinely checked before being entered into the data base. The measurements were edited, checked for gross errors, internal consistency of the data pertaining to each voyage, and climatic limits. Additional

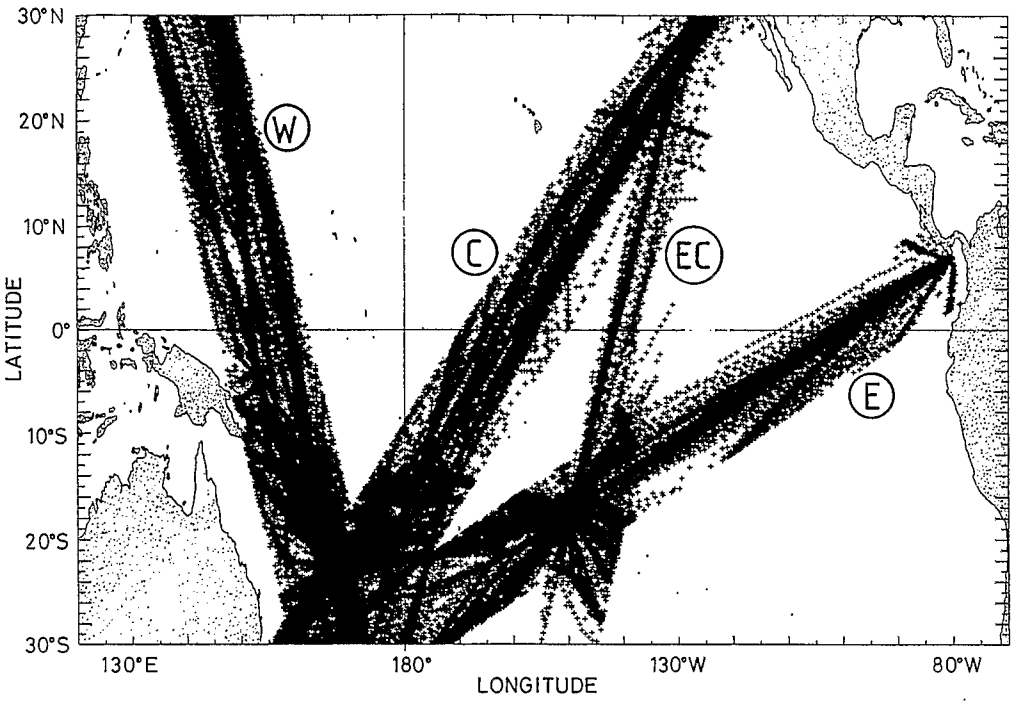

Fig. 1. Spatial distribution of sea surface temperature data collected along four mean shipping tracks in the tropical Pacific over the period 1969–1991 period. From west to east, these tracks are referred to as the western track (W), the central track (C), the east-central track (EC), and the eastern track (E) throughout the paper.

validation tests were applied to the selected SST values. Along each track, spurious SST measurements were detected through objective criteria based on multiples (±5, ±4, and then ±3.5) of sample standard deviations computed in 2° latitude bands. This procedure resulted in the loss of about 1% of the SST observations. In what follows, the time–latitude distribution of the validated SST measurements (Fig. 2) should be kept in mind. Results concerning variability in regions where the number of observations is small should be viewed with caution. Note that all the measurements to be analysed end in December 1991, whereas they start at different times: in August 1969, August 1975, May 1976 and September 1974, for the western (56,900 observations), central (38,600), east-central (13,000) and eastern (30,900) tracks, respectively.

As shown in Fig. 2, the along-track SST data are irregularly distributed in latitude and time; they were therefore interpolated onto regular one month by 2° latitude (e.g. 1°N–1°S) grids by an objective interpolation scheme (Laplacian method). On average, a grid element represents 8.2, 6.7, 3.1 and 8.1 measurements, for the western, central, east-central and eastern tracks, respectively. The gridded SST values were then smoothed (Laplacian smoothing), and a 1/4, 1/2, 1/4 filter was applied on each time series. This processing procedure is identical to the one used by DELCROIX and HÉNIN (1991) in a companion paper dealing with sea surface salinity data.

Estimation of the errors induced by the use of bucket measurements already has been amply documented (cf. REVERDIN *et al.*, 1988, and its references). Comparisons between

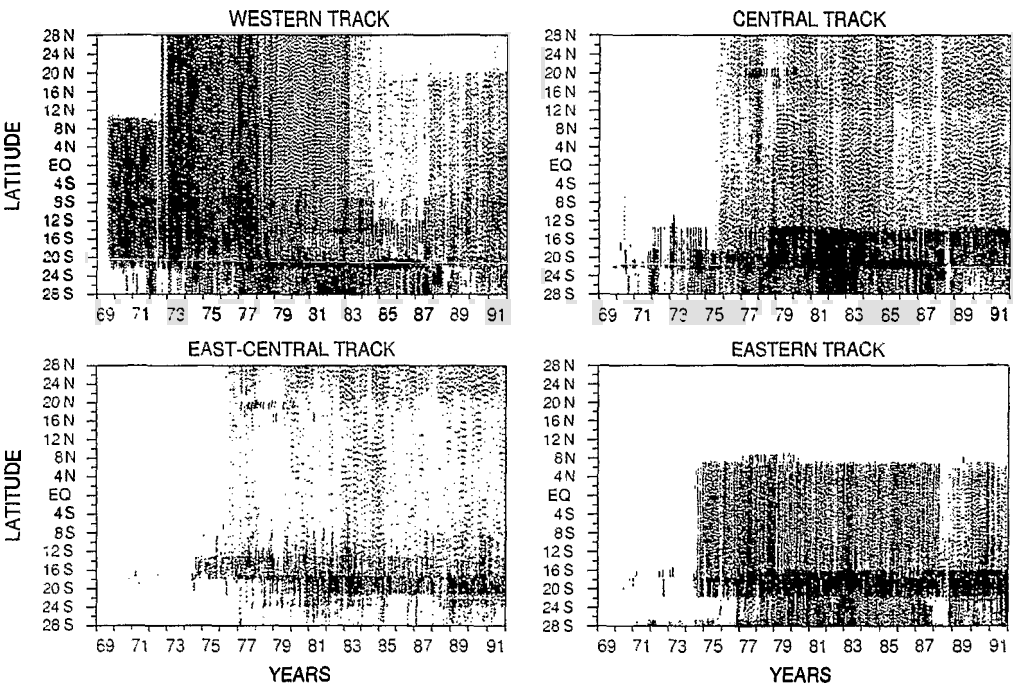

Fig. 2. Time–latitude distribution of sea surface temperature data for the four selected tracks.

bucket and other *in situ* SST measurements are difficult to interpret as the data are rarely simultaneous in space and time. An error estimate was made by comparing bucket SST, collected so as to approximate SOP situation, with simultaneous CTD measurements obtained during ORSTOM–SURTROPAC research cruises in the western tropical Pacific. For the 173 comparisons made during 1989–1992, the mean (bucket minus CTD) and rms differences between bucket and CTD measurements obtained from these cruises were −0.15°C and 0.37°C, respectively. Given that CTD is a very accurate instrument, this provides an order of magnitude of the expected bias and accuracy of a bucket SST. However, precision in a gridded SST value depends on the multiple processing stages applied to the raw data. On a mean, a gridded SST value represents 6.5 observations collected during a given month, within a 2° latitude by 10–20° longitude band. Although the rms error is reduced roughly by a factor of $6.5^{1/2}$, inadequate sampling in a month and a 2° latitude band, and the effect of grouping the scattered SST data into a mean track, may still alter precision in a gridded value. For all these reasons, the overall accuracy of the gridded SST fields is probably not better than 0.3°C.

ANNUAL MEAN AND SEASONAL VARIABILITY

As noted by MEYERS (1982), by excluding the ENSO years in the tropical Pacific thermal structure, it is possible to construct means that fall into Gaussian distributions. The long-term annual mean of SST is thus calculated from the monthly gridded values, excluding the 1972–1973, 1976, 1982–1983 and 1987 ENSO years as defined by QUINN *et al.* (1987).

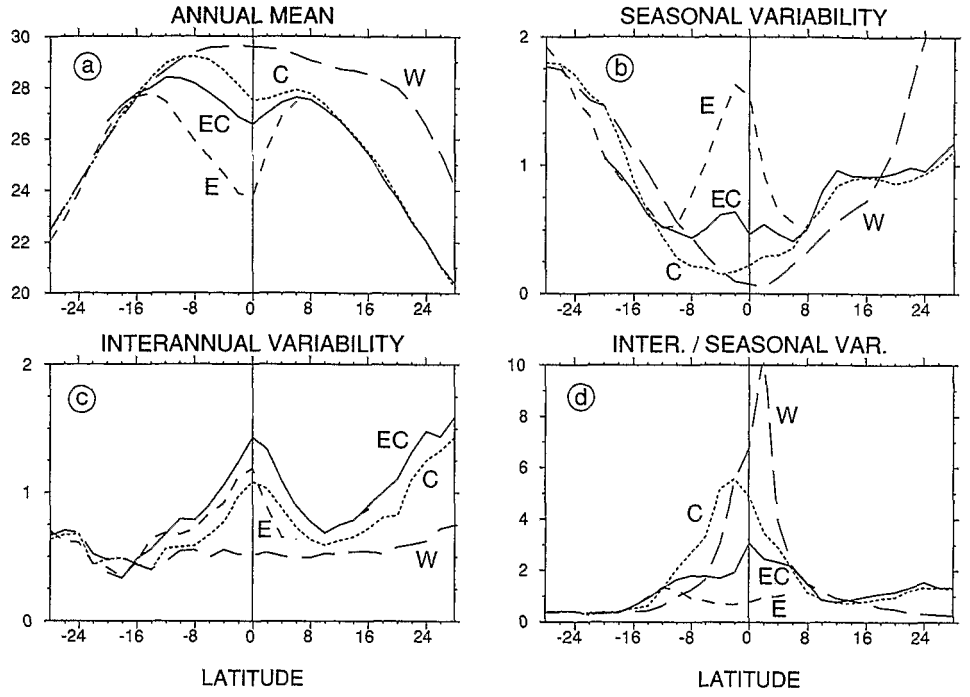

Fig. 3. (a) Annual mean (°C), (b) seasonal variability (°C), (c) interannual variability (°C), and (d) interannual vs seasonal variability of sea surface temperature for the western (W), central (C), east-central (EC) and eastern (E) tracks.

Similarly, a mean year is constructed by omitting the ENSO years; the standard deviation (σ_s) of the 12 mean months is used as a measure of the seasonal variability.

The long-term annual means of SST are presented in Fig. 3a. Maximum SST values (>29°C) are located along the western track, between 10°S and 8°N, decreasing poleward and toward the east. The SST warmer than 28°C, temperature threshold frequently used to delimit the warm pool region, is found along the western, central, and east-central tracks, within 14°S–18°N, 14°S–2°N, and 12–8°S, respectively. Except along the western track, local SST maxima appear on either side of, but asymmetrically about, the equator. The SST maxima at 6°N (155, 137 and 85°W), 8°S (170°W), 12°S (145°W) and 14°S (135°W) seem to be associated with the zonally-oriented Intertropical Convergence Zone (ITCZ) and the NW/SE-oriented South Pacific Convergence Zone (SPCZ). The way ITCZ and SPCZ are coupled to the underlying SST, however, is still an open question. Between the local maxima, a minimum SST lies on the equator, characterizing the progressive appearance of the equatorial upwelling to the east. These annual means in SST agree closely with the results of Horel (1982) and Levitus (1982).

The amplitude (σ_s) of the seasonal variability in SST increases poleward in each hemisphere from 8–10° latitude (Fig. 3b). The largest values are obtained for grids in the western Pacific, and in particular in the Kuroshio region (σ_s=2.8°C at 28°N). In the equatorial band, the seasonal variability is very slight ($\sigma_s < 0.25$°C) for the two western-most tracks and increases toward the east to reach 0.5°C at 140°W and 1.5°C at 100°W. This difference reflects the eastward increase of the seasonal signal in the equatorial upwelling

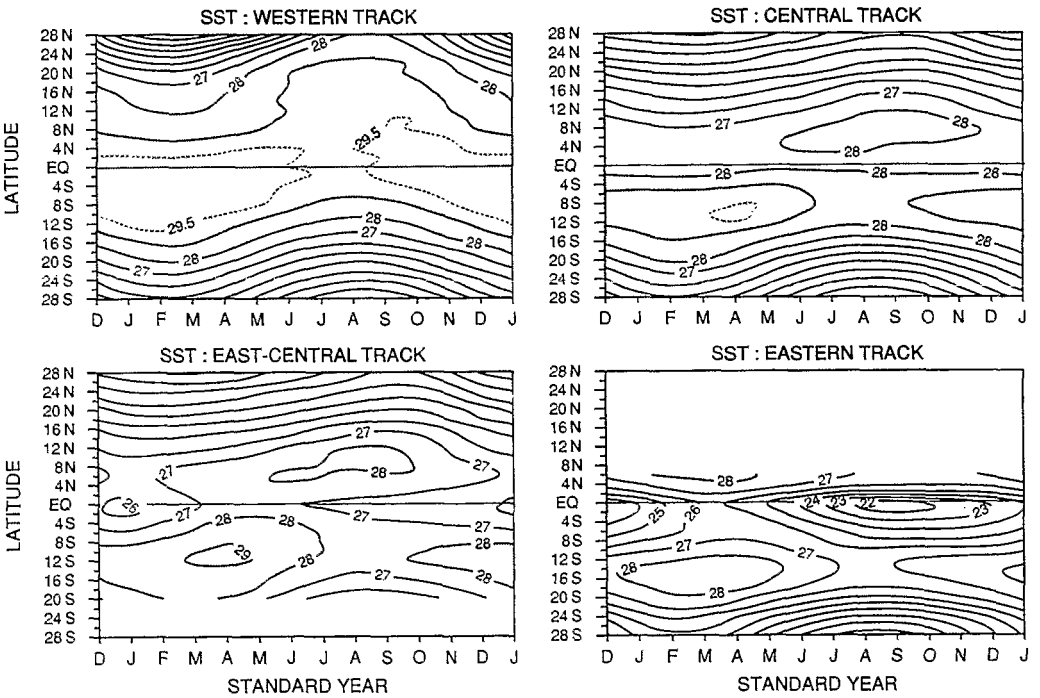

Fig. 4. Mean seasonal cycle of sea surface temperature for the four selected tracks. Contour intervals are 1°C, except for the dashed lines which denote the 29.5°C isotherm. Shaded areas represent sea surface temperature above 28°C.

extending from the date line to the Galapagos Islands. Note, however, that the maximum SST seasonal variability is not located right at the equator but slightly displaced southward, in agreement with the findings of WEARE *et al.* (1976).

As can be expected, away from the equatorial band, the SST is warmest (coldest) during the summer (winter) hemisphere (Fig. 4). This merely reflects the considerable impact of the surface thermal forcing in controlling extra-tropical SST (LIU and GAUTIER, 1990). In the equatorial band, the seasonal SST change is well-marked for the eastern track only. There, the SST is warmest during March–April when the ITCZ is farthest south and the zonal winds at the equator are at their weakest resulting in a minimum-strength upwelling. Conversely, the SST is coldest during September–October with the ITCZ is at its northernmost position, and when there are strong easterly winds (HASTENRATH and LAMB, 1977) and a westward surface current (HALPERN, 1987), yielding maxima in vertical and horizontal advections of cold water. In agreement with HOREL (1982), there is a suggestion on Fig. 4 that the seasonal SST warming moves westward from the equatorial eastern Pacific, the warmest equatorial SST being found in March–April at 100°W, May–June at 140°W, July–August at 160°W and January–February at 155°E. This is closely associated with the westward phase propagation of the seasonal signals in zonal winds (MEYERS, 1979) and zonal currents (MCPHADEN and TAFT, 1988). Strong interactions between the ocean and the atmosphere are obviously involved in the equatorial waveguide, at seasonal time scale.

As shown in Fig. 4, the seasonal SST signal at some latitudes can be easily represented

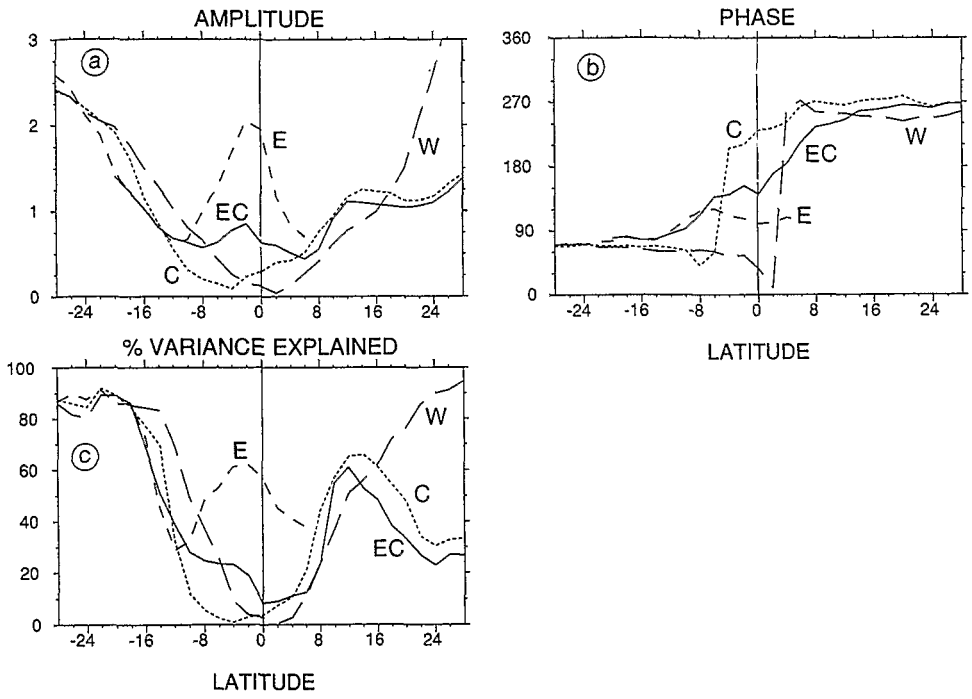

Fig. 5. Least squares fit to an annual harmonic of sea surface temperature for the western (W), central (C), east-central (EC) and eastern (E) tracks: (a) amplitude (°C), (b) year–day phase of warmest sea surface temperature, and (c) per cent of total variance explained by the fit.

by a periodic function of one year duration. For each track, least-squares fit to an annual harmonic was thus performed to assess how representative the annual SST cycle is of the total SST signal. The amplitude and phase of the annual harmonic, together with the percent of variance explained by the fit (Fig. 5) corroborate the previous discussion. The amplitude increases poleward from about 8° latitude, from east to west, and there is a 180° phase shift between the northern and southern hemispheres. In the equatorial band, the amplitude is negligible for the two westernmost tracks, and it reaches maximum values (2°C) at 2°S along the eastern track. Interestingly, the annual SST phase within 2–4° around the equator behaves more like the phase of the southern hemisphere for the western track, and more like the phase of the northern hemisphere for the central track. The reason for this is unclear. It is also noteworthy that there are regions near the equator where the annual SST cycle is not very significant: the annual SST cycle fits less than 20% of the total SST variance west of 140°W. In contrast, the annual cycle is a major signal in the eastern Pacific, accounting for at least 50% of the total variance. Because the annual cycle appears coupled with the interannual El Niño variability (Rasmusson and Carpenter, 1982), processes that govern its evolution, although only partly understood (Seager *et al.*, 1988), must be precisely quantified.

INTERANNUAL VARIABILITY

In the previous section, we mentioned regions where the annual SST cycle explains only a small part (<20%) of the total SST variance. To ascertain the relative contributions of

interannual vs seasonal SST changes, we computed anomalies of SST with reference to the 12 mean months; the standard deviation (σ_i) of these anomalies was used as a measure of the interannual SST variability. Estimates of the amplitude of the seasonal with respect to the interannual signals were obtained by computing the ratio (σ_i/σ_s) of the standard deviation of the interannual variability (σ_i) to the standard deviation of the seasonal variability (σ_s).

The interannual variability of SST (Fig. 3c) is distributed fairly similarly along the three easternmost tracks. Within 10° off the equator, σ_i can be roughly represented by a Gaussian function with the acme at the equator (σ_i = 1–1.5°C). Such a distribution does not conflict with model results indicating that interannual El Niño-related variability might stem from anomalous equatorially-trapped eastward surface advection associated with long equatorial waves (HARRISON and SCHOPF, 1984). Further poleward, σ_i increases in regions where the meridional gradient in mean SST is high (i.e. in thermal frontal zones). Along the western track, the interannual variability is almost constant, ranging from 0.5 to 0.75°C. Obviously, high values of the ratio (σ_i/σ_s) are found in the regions where the seasonal SST signal is weak. As shown in Fig. 3d, notable track to track (i.e. almost zonal) variations of (σ_i/σ_s) are found mainly within 8°N–8°S, particularly near the equator where the ratio gradually increases from east to west. This feature clearly illustrates one fundamental difference in SST changes between the western equatorial Pacific, where interannual variations exceed seasonal variations, and the eastern equatorial Pacific, where interannual and seasonal variations are of the same order of magnitude.

Having presented a brief description of the interannual SST changes, we shall now examine time series of sea surface temperature anomalies (SSTA), between 20°S and 20°N to highlight the basin-scale features (Fig. 6), and at the equator, to better apprehend the timing of the anomalies (Fig. 7). Bear in mind that "at the equator" signifies the mean for 1°N–1°S.

Looking at the eastern track in Fig. 6, we see that significant positive SSTA, exceeding 0.5–1°C, appear during five remarkable periods that characterize the 1976 moderate El Niño event, the 1979 aborted event, the 1982–1983 very strong event, the 1987 moderate event, and the premise of the 1991–1992 event (QUINN *et al.*, 1987; DONGUY and DESSIER, 1983; ENFIELD *et al.*, 1992). El Niño-related SSTA also can be traced along both the poorly-sampled east-central track (except in 1976) and the central track, reflecting the basin-scale impact of El Niño events. In agreement with Fig. 3c, positive SSTA warmer than 1°C appear somewhat trapped at the equator, extending on a mean from 8°N–8°S. As noted previously, this is perhaps in relation with the signature of equatorially-trapped surface current anomalies associated with equatorial waves. Only detectable along the eastern track, negative SSTA occur near the end of 1975 at a time of positive Southern Oscillation Index (SOI) (Climate Analysis Center, Washington D.C., U.S.A.). In the second half of 1983, negative SSTA exist near the equator for the east-central and central tracks, in agreement with other data sets (HARRISON *et al.*, 1990). As was to be expected, the strong 1988–1989 La Niña event results in well-marked negative SSTA (<−2°C) for the three easternmost tracks. (Note the lack of data between March and October 1988 along the eastern track.)

Because SSTA are generally maximal at the equator, their timing and amplitude can be more easily traced using Fig. 7. Note that from west to east, the selected tracks cross the equator near 155°E and 160, 140 and 100°W. The 1976 moderately strong El Niño event results in above normal equatorial SSTA from April 1976 to March 1977 near 100°W, and

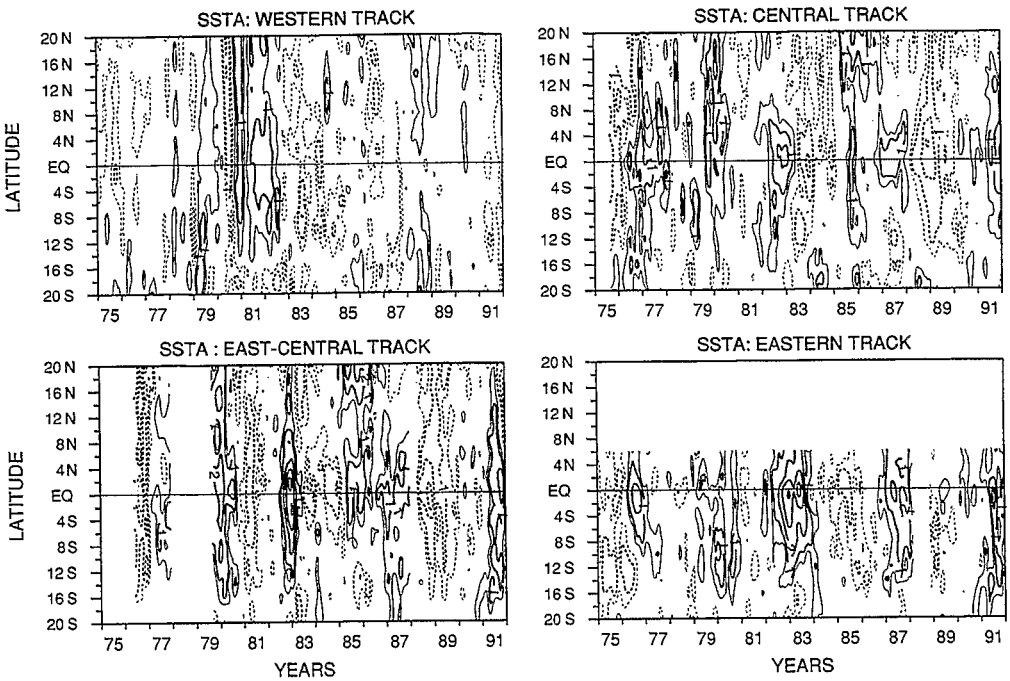

Fig. 6. Time–latitude diagrams of sea surface temperature anomalies relative to the mean seasonal cycles. Contour intervals are 1°C, except for the ±0.5°C anomalies. The zero contour is dropped for clarity, and the dashed lines denote negative anomalies. Shaded areas represent sea surface temperature anomalies above 0.5°C.

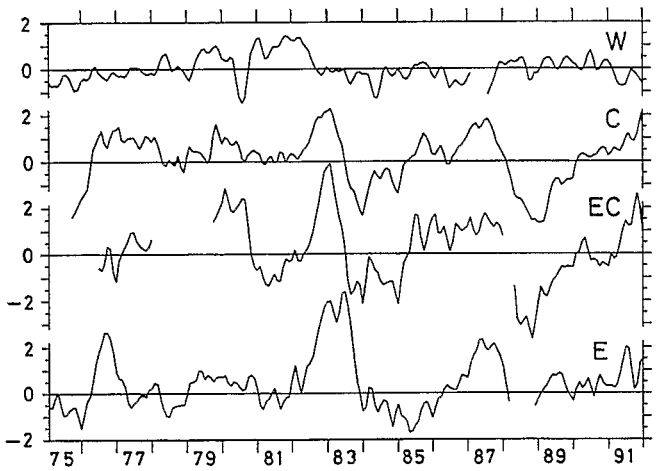

Fig. 7. Equatorial sea surface temperature anomalies (°C) relative to the mean seasonal cycles, for the western (W), central (C), east-central (EC) and eastern (E) tracks.

from April 1976 to early 1978 near 160°W. (Note that the lack of the El Niño signal near 140°W may reflect the poor data coverage along the east-central track.) Maximum equatorial SSTA are reached in August 1976 near 100°W (2.7°C), and in January 1977 near 160°W (1.5°C). This is in qualitative agreement with the SSTA along the coast off Peru, as reported in WYRTKI (1979).

DONGUY and DESSIER (1983) have reported the occurrence of a very weak El Niño during 1979, from sea surface salinity and temperature data collected along the same tracks as in Fig. 1. Figure 7 shows that positive SSTA occur during some months in 1979 and 1980 near 100, 140 and 160°W. It should be noted that three month periods with SSTA warmer than 1°C only appear along the poorly-sampled east-central track. SSTA derived from operational products (Climate Analysis Center, Washington, D.C., U.S.A.) in NIÑO 1+2 (0–10°S; 80–90°W), NIÑO 3 (6°N–6°S; 90–150°W), and NIÑO 4 (6°N–6°S; 150°W–160°E) regions never exceed 1°C during 1979–1980.

In the western equatorial Pacific, prior to the very strong 1982–1983 event, there is a trend for SSTA to increase from 1975 to early 1982 (about 0.25°C y^{-1}) (Fig. 7). There, SSTA warmer than 1°C only happen in 1981 and early 1982, which is consistent with the results reported by MEYERS *et al.* (1986), based on XBT data. Whether this warming was significant and/or instrumental in setting the stage for the strongest event on record is not clear. Positive equatorial SSTA are observed during the first quarter of 1982, almost simultaneously near 100, 140 and 160°W. There is no clear evidence, with the present data set, that SSTA first occur in the western equatorial Pacific and subsequently propagate eastward, as suggested by GILL and RASMUSSON (1983). The warmest equatorial SSTA occur in both January (4°C) and June (4.4°C) 1983 near 100°W, and in January 1983 near 140°W (3.9°C) and 160°W (2.3°C). Interestingly, the SSTA near 100°W present two distinct peaks (January and June 1983), in qualitative agreement with the El Niño composite of RASMUSSON and CARPENTER (1982) except that the present episode started several months earlier and lasted longer than the composite. This double peak structure may reflect the signature of first-baroclinic mode Kelvin waves (CANE, 1984): the first peak is primarily due to the changes in the winds close to the dateline, the second peak results from the collapse of the trade winds in the central Pacific. However, the cause and effect relations of Kelvin wave-induced anomalous advection and warm SST are still insufficiently understood. From mid-1983, the equatorial SST decreases, returning to normal in October 1983 near 100°W, and in July 1983 near 140 and 160°W. The warm 1982–1983 episode has ended, and the eastern half of the equatorial Pacific becomes colder than normal in 1984 and part of 1985. All these findings agree reasonably well with the large-scale pattern of SST evolution in 1982–1983, in particular with near-surface 110°W mooring data (HALPERN, 1987) and with XBT measurements along the central track (TOURNIER, 1989).

During the 1986–1987 El Niño event, the positive equatorial SSTA begins in mid-1986 near 100, 140 and 160°W and remains above normal throughout 1987 (Fig. 7). The largest positive equatorial SSTA occur both in May (2.3°C) and September (2.2°C) 1987 near 100°W, and in June 1987 near 140°W (1.7°C) and 160°W (1.8°C). As during a canonical El Niño, there is a double peak in SSTA structure in the east, although variations between May and September 1987 approach the measurement accuracy. Equatorial SSTA remains above normal, decreasing from mid-1987 to January 1988. Then from February to the end of 1988, equatorial SSTA drop by 3–4°C near 140 and 160°W (no data near 100°W) as the 1986–1987 El Niño warm event give way to a cold La Niña lasting to the end of 1989.

Despite quantitative disagreements of the order of 1°C, our time evolution of equatorial SSTA during the 1986–1988 period is supported by McPHADEN and HAYES (1990), who used equatorial mooring SST data at 110 and 140°W. Quantitative disagreements may reflect the different type of measurements, the use of different climatologies, and the fact that the present SSTA represent means over 2° latitude by 10–20° longitude boxes not strictly centred around mooring locations.

Finally, equatorial SSTA warmer than 0.5–1°C happen in mid-1991 near 160, 140 and 100°W: they evidence the early effects of the 1991–1992 El Niño. The beginning of the event only is captured here; SSTA seem in agreement with operational products (Climate Analysis Center, Washington, D.C., U.S.A.). Full descriptions of the event should be available soon.

Acknowledgements—Numerous officers and crews of merchant and navy ships voluntarily participate in the ORSTOM ship-of-opportunity programme, collecting sea surface temperature measurements among other parameters. The present analysis represents the combined efforts of many ORSTOM colleagues, and in particular owes much to J. R. Donguy and C. Hénin in initiating and continuing the surface ship-of-opportunity programme. Programming support was mainly provided by F. Masia. All these contributions are gratefully acknowledged.

REFERENCES

CANE M. (1984) Modeling sea level during El Niño. *Journal of Physical Oceanography*, **14**, 1864–1874.

DELCROIX T. and C. HÉNIN (1991) Seasonal and interannual variations of sea surface salinity in the tropical Pacific Ocean. *Journal of Geophysical Research*, **96**, 22135–22150.

DONGUY J. R. and A. DESSIER (1983) El Niño-like events observed in the tropical Pacific. *Monthly Weather Review*, **111**, 2136–2139.

ENFIELD D. B., R. CALIENES and L. PIZARRO (1992) Oceanographic conditions along the coast of south America during the 1991-92 El Niño/Southern oscillation. *TOGA Notes*, **8**, 1–4.

GILL A. and E. RASMUSSON (1983) The 1982–83 climate anomaly in the equatorial Pacific. *Nature*, **305**, 229–234.

HALPERN D. (1987) Observations of annual and El Niño thermal and flow variations at 0–110°W and 0–95°W during 1980–1985. *Journal of Geophysical Research*, **92**, 8197–8212.

HARRISON D. E. and P. S. SCHOPF (1984) Kelvin-wave induced anomalous advection and the onset of surface warming in El Niño events. *Monthly Weather Review*, **112**, 913–933.

HARRISON D. E., B. S. GIESE and E. S. SARACHIK (1990) Mechanisms of SST change in the equatorial waveguide during the 1982–83 El Niño. *Journal of Climate*, **3**, 173–188.

HASTENRATH S. and P. J. LAMB (1977) *Climatic atlas of the tropical Atlantic and eastern Pacific oceans*. 97 charts. University of Wisconsin Press, Madison.

HAYES S., P. CHANG and M. J. MCPHADEN (1991) Variability of the sea surface temperature in the eastern equatorial Pacific during 1986-1988. *Journal of Geophysical Research*, **96**, 10553–10566.

HOREL J. (1982) On the annual cycle of the tropical Pacific atmosphere and ocean. *Monthly Weather Review*, **110**, 1863–1878.

LEVITUS S. (1982) *Climatological atlas of the world ocean*. NOAA Professional Paper, 173 pp, U.S. Govt. Print. Off., Washington D.C.

LIU T. and C. GAUTIER (1990) Thermal forcing on the tropical Pacific from satellite data. *Journal of Geophysical Research*, **95**, 13209–13217.

MCPHADEN M. J. and S. P. HAYES (1990) Variability in the eastern equatorial Pacific ocean during 1986–1988. *Journal of Geophysical Research*, **95**, 13195–13208.

MCPHADEN M. J. and B. A. TAFT (1988) Dynamics of seasonal and intraseasonal variability in the eastern equatorial Pacific. *Journal of Physical Oceanography*, **18**, 1713–1732.

MCPHADEN M. J., F. BAHR, Y. DUPENHOAT, E. FIRING, S. P. HAYES, P. P. NIILER, P. L. RICHARDSON and J. TOOLE (1992) The response of the western equatorial Pacific ocean to westerly wind burst forcing: November 1989–January 1990. *Journal of Geophysical Research*, **97**, 14289–14303.

MEYERS G. (1979) Annual variation in the slope of the 14°C isotherm along the equator in the Pacific ocean. *Journal of Physical Oceanography*, **9**, 885–891.

MEYERS G. (1982) Interannual variation in sea level near Truk Island: A bimodal seasonal cycle. *Journal of Physical Oceanography*, **12**, 1161–1168.

MEYERS G., J. R. DONGUY and R. K. REED (1986) Evaporative cooling of the western equatorial Pacific Ocean by anomalous winds. *Nature*, **323**, 523–526.

PAN Y. H. and A. H. OORT (1983) Global climatic variations connected with sea surface temperature anomalies in the eastern Pacific ocean for the 1958–1973 period. *Monthly Weather Review*, **111**, 1244–1258.

PALMER T. and D. A. MANSFIELD (1984) Response of two atmospheric general circulation models to sea surface temperature anomalies in the tropical east and west Pacific. *Nature*, **310**, 483–485.

QUINN W. H., V. T. NEAL and S. E. ANTUNEZ DE MAYOLO (1987) El Niño occurrences over the past four and a half centuries. *Journal of Geophysical Research*, **92**, 14449–14461.

RASMUSSON E. M. and T. H. CARPENTER (1982) Variations in tropical sea surface temperature and surface wind field associated with the southern Oscillation/El Niño. *Monthly Weather Review*, **110**, 354–384.

REVERDIN G., Y. DUPENHOAT and J. SERVAIN (1988) Sea surface temperature: a comparison between ship reports from marine decks and ship-of-opportunity subsurface data in the tropical Atlantic ocean. *Tropical Ocean–Atmosphere Newsletter*, **47**, 1–4.

REYNOLDS R. W. (1988) A real-time global sea surface temperature analysis. *Journal of Climate*, **1**, 75–86.

SEAGER R. (1989) Modeling tropical Pacific sea surface temperature: 1970–1987. *Journal of Physical Oceanography*, **19**, 419–434.

SEAGER R., S. E. ZEBIAK and M. A. CANE (1988) A model of the tropical Pacific sea surface temperature climatology. *Journal of Geophysical Research*, **93**, 1265–1280.

TOURNIER R. (1989) Variabilité de la structure thermique et des courants à l'ouest et au centre de l'océan Pacifique tropical. Thèse de doctorat, 154 pp, Université de Paris VI, Paris.

WEARE B. C., A. R. NAVATO and R. E. NEWELL (1976) Empirical orthogonal analysis of Pacific sea surface temperature. *Journal of Physical Oceanography*, **6**, 671–678.

WHITE W. B., G. MEYERS, J. R. DONGUY and S. E. PAZAN (1985) Short-term variability in the thermal structure of the Pacific ocean during 1979-82. *Journal of Physical Oceanography*, **15**, 917–935.

WORLD CLIMATE RESEARCH PROGRAM (1985) Scientific plan for the Tropical Ocean and Global Atmosphere program, Publ. 3, World Meteorological Organization, Geneva, 146 pp.

WYRTKI K. (1979) The response of the sea surface topography to the 1976 El Niño. *Journal of Physical Oceanography*, **9**, 1223–1231.